Synthesis and Characterization of Tetraruthenaborane Clusters: Molecular Structure of $[HRu_4(CO)_{12}Au_2(PPh_3)_2B]$

Ann K. Chipperfield and Catherine E. Housecroft*

University Chemical Laboratory, Lensfield Road, Cambridge CB2 1EW, U.K.

Arnold L. Rheingold*

Department of Chemistry, University of Delaware, Newark, Delaware 19716

Received July 24, 1989

The tetraruthenaborane cluster $HRu_4(CO)_{12}BH_2$ (1) has been synthesized and characterized spectroscopically. Deprotonation to $[HRu_4(CO)_{12}BH]^-$ (2) occurs via the loss of an Ru–H–B bridging proton. Compounds 1 and 2 are structural analogues of the ferraboranes $HFe_4(CO)_{12}BH_2$ and $[HFe_4(CO)_{12}BH]^-$, although, compared to $[HFe_4(CO)_{12}BH]^-$, 2 exhibits a higher activation barrier for *endo*-hydrogen exchange, in line with the increased M–H–M and M–H–B bond energies in going from M = Fe to Ru. The reaction of 2 with PPh_3AuCl leads to $HRu_4(CO)_{12}Au(PPh_3)BH$ (3) and $HRu_4(CO)_{12}Au_2(PPh_3)_2B$ (4), and as one progresses across the series of clusters 1–4, the boron atom is converted from a borane to a borido environment. The tetraruthenium butterfly framework present in compounds 1–4 has been confirmed by a single-crystal X-ray crystallographic characterization of 4: triclinic, $P\bar{1}$, a = 13.212 (3) Å, b = 13.366 (3) Å, c = 15.261 (4) Å, α = 96.92 (2)°, β = 94.40 (2)°, γ = 103.91 (2)°, V = 2581.2 (10) Å^3, Z = 2, R_F = 3.94%. The structure of 4 is similar to that found for $HFe_4(CO)_{12}Au_2(PEt_3)_2B$ but differs significantly from that of $Fe_4(CO)_{12}Au_2(PPh_3)_2BH$. Subtle differences between the carbonyl orientations in 4 and $HFe_4(CO)_{12}Au_2(PEt_3)_2B$, and between the exact geometries of the M_4Au_2B cores (M = Fe, Ru) in the two compounds, support our earlier postulates regarding the sterically controlled pathway for isomer interconversion between $Fe_4(CO)_{12}Au_2(PR_3)_2BH$ and $HFe_4(CO)_{12}Au_2(PR_3)_2B$ (R = alkyl, aryl), a pathway that involves hydrogen atom migration triggered by a rearrangement of the gold(I) phosphine groups and reorientation of one $\{Fe(CO)_3\}$ fragment.

Introduction

Investigations of the interactions of main-group elements with tetranuclear transition-metal butterfly clusters represent a rapid growth area in inorganic cluster chemistry, in particular because the butterfly array of metal atoms represents a molecular model for a "stepped", catalytically active site on a metal surface.[1] Recently, our attention has focused on the chemistry of ruthenaborane clusters, with an emphasis on clusters in which the ratio of metal to boron atoms is ≥2.[2,3] Clusters containing a tetraruthenium butterfly core are now well documented,[1] and of these, compounds in which the Ru_4 butterfly interacts with a main-group element exemplify Ru–C,[4,5] Ru–N,[6–9] Ru–P,[10] and Ru–Cl[11] bond formation. In the case of the carbido and nitrido clusters, the main-group atom interacts with all four metal atoms of the Ru_4 framework, while in the Ru_4P core the phosphorus atom is in a μ_3-bonding mode and in the Ru_4C core the chlorine atom interacts only with the wingtip ruthenium atoms. The ruthenaborane $HRu_4(CO)_{12}BH_2$ has previously been reported by Lewis and Johnson et al., and on the basis of infrared, mass, and ^1H NMR spectroscopic data, it was proposed that the cluster possessed either a tetrahedral or butterfly Ru_4 core.[12] Subsequently, Fehlner et al. established that the structure of the analogous ferraborane $HFe_4(CO)_{12}BH_2$ comprised an Fe_4 butterfly framework.[13] We have now confirmed the presence of an Ru_4 butterfly in $HRu_4(CO)_{12}BH_2$; the boron atom resides within the interstice of the metal butterfly, while retaining interactions to two *endo*-hydrogen atoms. The boridic nature of the boron atom is enhanced by replacing these *endo*-hydrogen atoms with gold(I) phosphine fragments. In the discussion below, we shall delineate the rather subtle differences observed between the geometries of the M_4Au_2B core in $HM_4(CO)_{12}Au_2(PPh_3)_2B$ for M = Fe[14,15] and Ru.

Experimental Section

General Data. FT-NMR spectra were recorded on a Bruker WM 250 or AM 400 spectrometer. ^1H NMR shifts are reported with respect to δ = 0 for Me_4Si, ^{11}B NMR with respect to δ = 0 for $F_3B{\cdot}OEt_2$, and ^{31}P NMR with respect to δ = 0 for H_3PO_4. All downfield chemical shifts are positive. Infrared spectra were recorded on a Perkin-Elmer FT 1710 spectrophotometer. Mass spectra were recorded on a Kratos MS 890 instrument.

All reactions were carried out under argon by using standard Schlenk techniques.[16] Solvents were dried over suitable reagents and freshly distilled under nitrogen before use. The products were

(1) Sappa, E.; Tiripicchio, A.; Carty, A. J.; Toogood, G. E. *Prog. Inorg. Chem.* **1987**, *35*, 437.
(2) Chipperfield, A. K.; Housecroft, C. E. *J. Organomet. Chem.* **1988**, *349*, C17.
(3) Chipperfield, A. K.; Housecroft, C. E.; Raithby, P. R. *Organometallics*, in press.
(4) Cowie, A. G.; Johnson, B. F. G.; Lewis, J.; Raithby, P. R. *J. Organomet. Chem.* **1988**, *306*, C63.
(5) Adams, R. D.; Babin, J. E.; Tanner, J. T. *Organometallics* **1988**, *7*, 765.
(6) Collins, M. A.; Johnson, B. F. G.; Lewis, J.; Mace, J. M.; Morris, J.; McPartlin, M.; Nelson, W. J. H.; Puga, J.; Raithby, P. R. *J. Chem. Soc., Chem. Commun.* **1983**, 689.
(7) Braga, D.; Johnson, B. F. G.; Lewis, J.; Mace, J. M.; McPartlin, M.; Nelson, W. J. H.; Puga, J.; Raithby, P. R.; Whitmire, K. H. *J. Chem. Soc., Chem. Commun.* **1982**, 1081.
(8) Blohm, M. L.; Gladfelter, W. L. *Organometallics* **1985**, *4*, 45.
(9) Blohm, M. L.; Gladfelter, W. L. *Inorg. Chem.* **1987**, *26*, 459.
(10) MacLaughlin, S. A.; Carty, A. J.; Taylor, N. J. *Can. J. Chem.* **1982**, *60*, 87.
(11) Steinmetz, G. R.; Harley, A. D.; Geoffroy, G. L. *Inorg. Chem.* **1980**, *19*, 2985.
(12) Eady, C. R.; Johnson, B. F. G.; Lewis, J. *J. Chem. Soc., Dalton Trans.* **1977**, 477.
(13) Wong, K. S.; Scheidt, W. R.; Fehlner, T. P. *J. Am. Chem. Soc.* **1982**, *104*, 1111. Fehlner, T. P.; Housecroft, C. E.; Scheidt, W. R.; Wong, K. S. *Organometallics* **1983**, *2*, 825.
(14) Housecroft, C. E.; Rheingold, A. L. *Organometallics* **1987**, *6*, 1332.
(15) Housecroft, C. E.; Shongwe, M. S.; Rheingold, A. L. *Organometallics* **1989**, *8*, 2651.
(16) Shriver, D. F.; Drezdon, M. A. *The Manipulation of Air-Sensitive Compounds*, 2nd ed.; Wiley: New York, 1986.

0276-7333/90/2309-0681$02.50/0

separated by thin-layer chromatography with Kieselgel 60-PF_{254} mesh (Merck). $Ru_3(CO)_{12}$ and PPh_3PAuCl were prepared from $RuCl_3 \cdot H_2O$ (Johnson-Matthey) and $HAuCl_4$ (Aldrich), respectively, by literature procedures.[17,18] Na_2CO_3, (PPN)Cl (PPN = bis(triphenylphosphine)nitrogen(1+)), and $THF \cdot BH_3$ were used directly as supplied by Aldrich.

Preparation of $HRu_4(CO)_{12}BH_2$ (1). $Ru_3(CO)_{12}$ (0.33 g, 0.52 mmol) was stirred in THF (16 mL) while Li[$BHEt_3$] (1 mL, 1 M solution in THF) followed by $THF \cdot BH_3$ (6 mL, 1 M solution in THF) was added. The solution was stirred at room temperature for 1.5 h, and then solvent was removed. Hexane (8 mL) and phosphoric acid (8 mL, 44% (aqueous)) were added to the solid residue. After the mixture was stirred for ~1 h, 10 mL of hexane was added to dilute the organic layer, which was subsequently removed from the acid by cannula. Product extraction was completed by using further portions of hexane (3 × 10 mL). Removal of solvent from the combined hexane solutions yielded a crude, red-brown solid. Product separation was achieved by using thin-layer chromatography with hexane eluent. Yellow $HRu_4(CO)_{12}BH_2$ was obtained as the fifth of six bands[19] in ~10% yield with respect to $Ru_3(CO)_{12}$ (40 mg 0.05 mmol): 250-MHz ^1H NMR ($CDCl_3$, 298 K) δ −8.4 (br q, J_{BH} = 65 Hz, Ru-*H*-B), −21.18 (s, Ru-*H*-Ru); 128-MHz ^{11}B NMR ($CDCl_3$, 298 K) δ 109.9 (t, J_{BH} = 70 Hz); IR (hexane, cm^{-1}) ν_{CO} 2074 vs, 2063 vs, 2051 m, 2030 s, 2017 w, 2003 w; EI-MS m/z 756 (P^+) with the loss of 12 CO's observed. Compound **1** is slightly air sensitive both in the solid and in solution.

Preparation of [PPN][$HRu_4(CO)_{12}BH$]. (PPN)Cl (0.07 mmol) was dissolved in MeOH (5 mL), and Na_2CO_3 (0.02 g, 0.17 mmol) was suspended in the solution. $HRu_4(CO)_{12}BH_2$ (0.05 mmol) was dissolved in acetone (5 mL), and the solution was added by cannula to the methanol suspension. An immediate color change from yellow to orange was observed. After the mixture was stirred for 15 min, the solvent was removed, leaving a crude orange residue from which [PPN][$HRu_4(CO)_{12}BH$] (typically 50 mg, 0.04 mmol; yield ~80%) was extracted by using 2 × 10 mL portions of Et_2O. [PPN][$HRu_4(CO)_{12}BH$]: 250-MHz ^1H NMR ($(CD_3)_2CO$, 298 K) δ 7.7–7.4 (m, PPN^+), −6.7 (br, Ru-*H*-B), −20.92 (s, Ru-*H*-Ru); 128-MHz ^{11}B NMR ($CDCl_3$, 298 K) δ 142.2 (d, J_{BH} = 80 Hz); IR (CH_2Cl_2, cm^{-1}) ν_{CO} 2024 vs, 2000 s, 1985 m, 1970 m, 1920 w; FAB-MS (3-NBA matrix) m/z 727 (P^- − CO).

Preparation of $HRu_4(CO)_{12}Au(PPh_3)BH$ (3). [PPN][$HRu_4(CO)_{12}BH$] (0.05 mmol) was dissolved in CH_2Cl_2 (6 mL) with $AuPPh_3Cl$ (0.03 g, 0.07 mmol) and $TlPF_6$ (0.02 g, 0.07 mmol). The solution was stirred for 45 min, during which time a color change from orange to green-brown was observed. The solvent was removed and the residue collected. Product separation was achieved by using thin-layer chromatography and eluting with n-C_6H_{14}–CH_2Cl_2 (1:1). Orange-brown $HRu_4(CO)_{12}Au(PPh_3)BH$ (**3**) was collected as the first band in ~20% yield (12 mg, 0.01 mmol). Eight other bands were obsd., each in insufficient quantity to characterize. Compound **3** is slightly air sensitive in solution. $HRu_4(CO)_{12}Au(PPh_3)BH$: 250-MHz ^1H NMR ($(CD_3)_2CO$, 298 K) δ 7.7–7.5 (m, Ph_3P), −4.7 (br, Ru-*H*-B), −20.86 (s, Ru-*H*-Ru); 128-MHz ^{11}B NMR ($(CD_3)_2CO$, 298 K) δ 137.2 (fwhm 152 Hz, $^{11}B\{^1H\}$ fwhm 119 Hz, $J_{BH} \approx 60$ Hz[21]); IR (hexane, cm^{-1}) ν_{CO} 2088 w, 2063 w, 2052 vs, 2030 w, 2014 m, 2005 w, 1982 w, 1970 w; FAB-MS (3-NBA matrix), m/z 1214 (P^+) with loss of 12 CO observed.

Preparation of $HRu_4(CO)_{12}Au_2(PPh_3)_2B$ (4). [PPN][$HRu_4(CO)_{12}BH$] (0.05 mmol) was prepared in situ and dissolved in CH_2Cl_2 (10 mL) with $AuPPh_3Cl$ (0.10 g, 0.21 mmol) and $TlPF_6$ (0.02 g, 0.07 mmol). The solution was stirred for ~1 h, during which time a color change from orange to brown was observed. The solvent was removed and the residue collected. Products were separated by using thin-layer chromatography, with n-C_6H_{14}–CH_2Cl_2 (1:1) as eluent. Red $HRu_4(CO)_{12}Au_2(PPh_3)_2B$ (**4**) was collected as the third band from the top of the plate in ~70% yield (58 mg, 0.035 mmol). Six other bands were observed, but none was in sufficient quantity to characterize. Compound **4** is moderately air stable. $HRu_4(CO)_{12}Au_2(PPh_3)_2B$: 250-MHz ^1H NMR ($(CD_3)_2CO$, 298 K) δ 7.8–7.6 (m, *PPN*$^+$), −20.66 (s, Ru-*H*-Ru); 128-MHz ^{11}B NMR ($(CD_3)_2CO$, 298 K) δ 170.0; IR (hexane, cm^{-1}) ν_{CO} 2069 m, 2036 s, 2024 vs, 2009 w, 1988 m, 1951 w; FAB-MS (3-NBA matrix) m/z 1670 (P^+). Anal. Calcd for $Au_2BC_{48}H_{31}O_{12}P_2Ru_4$: C, 34.51; H, 1.87; P, 3.71. Found: C, 34.24; H, 1.75; P, 3.79.

Table I. Comparison of the ^1H and ^{11}B NMR Spectroscopic Properties of $HM_4(CO)_{12}BH_2$ and $[HM_4(CO)_{12}BH]^-$ (M = Fe, Ru)

compd	^1H NMR, δ M-H-B	^1H NMR, δ M-H-M	^{11}B NMR, δ	ref
$HFe_4(CO)_{12}BH_2$ (5)	−11.9	−24.9	+116	13
$HRu_4(CO)_{12}BH_2$ (1)	−8.4	−20.18	+109.9	this work, 23
$[HFe_4(CO)_{12}BH]^-$ (6)	−8.5	−24.9	+150	22[a]
$[HRu_4(CO)_{12}BH]^-$ (2)	−6.7	−20.92	+142.2	this work[a]

[a] Spectroscopic data reported for the PPN^+ salt.

Table II. Crystal Data for $HRu_4(CO)_{12}Au_2(PPh_3)_2B$ (4)

formula	$C_{48}H_{31}BO_{12}P_2Au_2Ru_4$
mol wt, M_r	1670.7
cryst syst	triclinic
space group	$P\bar{1}$
a, Å	13.212 (3)[a]
b, Å	13.366 (3)
c, Å	15.261 (4)
α, deg	96.92 (2)
β, deg	94.40 (2)
γ, deg	103.91 (2)
V, Å^3	2581.2 (10)
Z	2
D(calcd), g cm^{-3}	2.15
μ(Mo Kα), cm^{-1}	68.91
T, K	294
T_{max}/T_{min}	0.031/0.019
diffractometer	Nicolet R3m
radiation	Mo Kα (λ = 0.710 73 Å)
2θ limits, deg	$4 \le 2\theta \le 50$
data collected (hkl)	±16,±16,+19
rflns collected	9467
indpnt rflns	9095
R(int), %	4.29
obs rflns ($F_o \ge 3\sigma(F_o)$)	6939
std rflns (var)	3 std/197 rflns (~1%)
$R(F)$, %	3.94
R(wF), %	4.58
GOF	1.323
Δ/σ(max)	0.126
$\Delta(\rho)_{max}$, e Å^{-3}	2.2 (1.03 Å, Au(2))
N_o/N_v	12.62

[a] Unit cell parameters obtained from least-squares fit of the angular settings of 25 reflections ($20 \le 2\theta \le 28°$).

Crystal Structure Determination. Crystallographic data are collected in Table II. A deep red crystal (0.27 × 0.28 × 0.32 mm), obtained by recrystallization from CH_2Cl_2–hexane, was affixed to a glass fiber with epoxy cement. No evidence for lattice symmetry greater than triclinic was seen in photographic data or from cell reduction routines. The centrosymmetric alternative was selected initially and later affirmed by the chemical reasonableness of the results of refinement. Corrections for absorption were empirical (216 ψ-scan reflections). The two Au atoms were located by direct methods. All non-hydrogen atoms were refined anisotropically, and all H atoms (except for that bonded to Ru) were treated as idealized contributions (d_{CH} = 0.96 Å). The phenyl rings were constrained to rigid, planar hexagons (d_{CC} = 1.395 Å).

(17) Eady, C. R.; Jackson, P. F.; Johnson, B. F. G.; Lewis, J.; Malatesta, M. C.; MacPartlin, M.; Nelson, W. J. H. *J. Chem. Soc., Dalton Trans.* **1980**, 383.

(18) Mann, F. G.; Wells, A. F.; Purdie, D. *J. Chem. Soc.* **1937**, 1828.

(19) The first five bands from the top of the TLC plate were yellow-orange: band 1 = $H_3Ru_3(CO)_9CR$ (R = H, Me); band 2 = uncharacterized; band 3 = $H_2Ru_3(CO)_9C_2H_2$ and $Ru_3(CO)_9BH_5$;[2] band 4 = $Ru_3(CO)_{12}$, $H_4Ru_4(CO)_{12}$, and $Ru_3(CO)_9B_2H_6$[20] band 5 = 1. Band 6 was red and was identified as $H_2Ru_4(CO)_{13}$.

(20) Chipperfield, A. K.; Housecroft, C. E.; Matthews, D. M. *J. Organomet. Chem.*, in press.

(21) Coupling constant estimated from line width analysis.

Table III. Atomic Coordinates (×10⁴) and Isotropic Thermal Parameters (Å² × 10³) for 4

	x	y	z	U[a]		x	y	z	U[a]
Au(1)	2430.2 (3)	7559.5 (3)	3266.0 (3)	39.3 (1)	C(23)	1421	4858	6113	83 (7)*
Au(2)	2431.4 (3)	8149.8 (4)	1533.4 (3)	41.4 (2)	C(24)	1228	5769	5857	90 (8)*
Ru(1)	3274.5 (7)	9628.1 (7)	3841.6 (6)	42.3 (3)	C(25)	1532	6078	5056	70 (6)*
Ru(2)	726.5 (7)	8890.7 (7)	1872.9 (6)	40.5 (3)	C(26)	2028	5476	4509	47 (4)*
Ru(3)	2604.5 (7)	10589.4 (7)	2382.5 (6)	45.8 (3)	C(31)	462 (6)	5279 (5)	2259 (5)	57 (5)*
Ru(4)	1189.5 (8)	9920.0 (7)	3667.8 (6)	45.2 (3)	C(32)	-433	4597	1783	83 (7)*
P(1)	2283 (2)	5820 (2)	3408 (2)	41 (1)*	C(33)	-566	3523	1734	83 (7)*
P(2)	3379 (2)	7376 (2)	567 (2)	40 (1)*	C(34)	196	3132	2161	85 (7)*
B	2041 (10)	8998 (10)	2794 (8)	42 (5)*	C(35)	1090	3814	2637	68 (6)*
O(1)	5367 (7)	9407 (9)	3247 (7)	95 (5)*	C(36)	1223	4887	2686	48 (4)*
O(2)	3286 (10)	8546 (9)	5486 (6)	104 (5)*	C(41)	3647 (6)	4903 (7)	2438 (5)	63 (5)*
O(3)	4300 (9)	11748 (8)	4949 (8)	102 (5)*	C(42)	4627	4733	2300	79 (7)*
O(4)	-774 (8)	10228 (8)	1390 (8)	89 (5)*	C(43)	5475	5134	2953	90 (8)*
O(5)	513 (8)	8036 (10)	-100 (7)	103 (6)*	C(44)	5342	5704	3745	95 (8)*
O(6)	-920 (8)	7115 (8)	2382 (8)	88 (5)*	C(45)	4361	5873	3883	72 (6)*
O(7)	1561 (9)	11404 (10)	849 (8)	101 (6)*	C(46)	3513	5473	3230	51 (4)*
O(8)	4381 (7)	10274 (8)	1314 (7)	78 (4)*	C(51)	3010 (7)	8626 (5)	-707 (4)	53 (5)*
O(9)	3968 (12)	12691 (9)	3280 (10)	137 (7)*	C(52)	2945	8892	-1562	66 (6)*
O(10)	-884 (9)	10564 (11)	3446 (8)	112 (6)*	C(53)	3163	8246	-2272	68 (6)*
O(11)	1989 (10)	11383 (10)	5416 (7)	114 (6)*	C(54)	3446	7334	-2127	72 (6)*
O(12)	276 (8)	8023 (8)	4550 (7)	86 (5)*	C(55)	3511	7068	-1272	67 (6)*
C(1)	4593 (10)	9461 (10)	3466 (8)	61 (5)*	C(56)	3292	7714	-562	46 (4)*
C(2)	3265 (11)	8944 (10)	4846 (8)	67 (5)*	C(61)	1878 (5)	5500 (5)	434 (5)	53 (5)*
C(3)	3907 (11)	10971 (10)	4524 (9)	67 (5)*	C(62)	1490	4422	237	64 (5)*
C(4)	-225 (9)	9746 (10)	1593 (9)	58 (5)*	C(63)	2161	3799	-1	69 (5)*
C(5)	629 (10)	8346 (11)	641 (8)	66 (5)*	C(64)	3221	4253	-43	72 (6)*
C(6)	-292 (10)	7775 (9)	2172 (9)	57 (5)*	C(65)	3608	5331	153	58 (5)*
C(7)	1906 (11)	11081 (11)	1424 (10)	70 (6)*	C(66)	2937	5955	392	45 (4)*
C(8)	3690 (10)	10313 (9)	1696 (9)	57 (5)*	C(71)	5550 (6)	8193 (6)	443 (4)	58 (5)*
C(9)	3479 (13)	11891 (11)	2945 (11)	81 (6)*	C(72)	6611	8427	760	68 (6)*
C(10)	-128 (11)	10306 (11)	3499 (9)	67 (6)*	C(73)	6918	8154	1574	68 (6)*
C(11)	1710 (12)	10866 (11)	4771 (10)	75 (6)*	C(74)	6164	7647	2073	69 (6)*
C(12)	623 (10)	8753 (10)	4226 (9)	60 (5)*	C(75)	5102	7413	1756	63 (5)*
C(21)	2220 (7)	4566 (6)	4765 (5)	59 (5)*	C(76)	4795	7686	942	47 (4)*
C(22)	1916	4257	5567	75 (6)*					

[a] Asterisks indicate equivalent isotropic U values, defined as one-third of the trace of the orthogonalized $\mathbf{U}_{ij}$ tensor.

Chart I

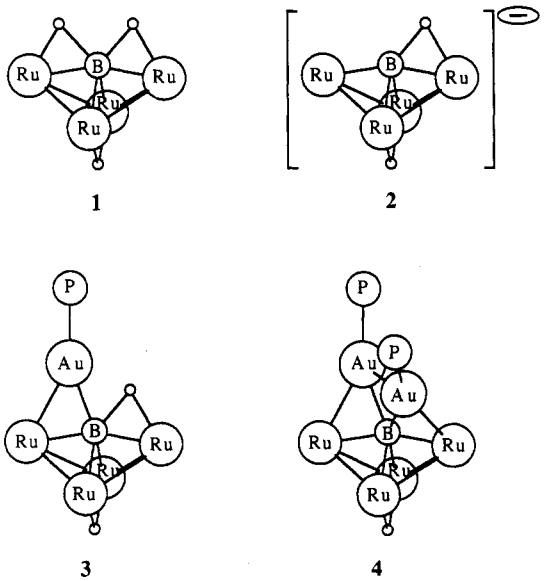

1 2 3 4

All computations used SHELXTL (5.1) software.[40] Table III gives the atomic coordinates, and Table IV gives selected bond distances and angles.

Results and Discussion

$HRu_4(CO)_{12}BH_2$ and $[HRu_4(CO)_{12}BH]^-$. One of the major boron-containing products from the reaction of $Ru_3(CO)_{12}$ and BH_3·THF in the presence of hydride ion is $HRu_4(CO)_{12}BH_2$ (1; Chart I). In a similar reaction, the iron carbonyls $Fe(CO)_5$ and $Fe_2(CO)_9$ react with BH_3·THF and hydride ion to give $HFe_4(CO)_{12}BH_2$ (5; Chart II).[22]

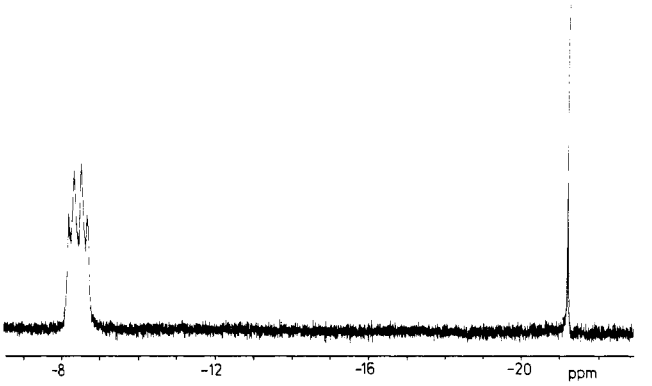

Figure 1. ^1H NMR spectrum (250 MHz, high-field region) of 1 illustrating Ru-H-B and Ru-H-Ru resonances.

The spectroscopic properties of 1 are consistent with this cluster possessing a structure analogous to that of 5. Preliminary spectroscopic data for 1 have previously been presented,[12,23] but the present results increase the amount of information available for this tetraruthenaborane cluster and allow the structural assignment to be confirmed. The ^1H NMR spectrum of 1 exhibits high-field resonances at δ −8.4 and −21.18 assigned to Ru-H-B and Ru-H-Ru protons, respectively (Figure 1). The collapsed quartet observed for the signal at δ −8.4 confirms that each of the

(22) Housecroft, C. E.; Buhl, M. L.; Long, G. J.; Fehlner, T. P. *J. Am. Chem. Soc.* **1987**, *109*, 3323.

(23) After our paper had been submitted, the ^{11}B NMR spectrum and a confirmation of the ^1H NMR spectrum of 1 were independently reported: Hong, F.-E.; Coffy, T. J.; McCarthy, D. A.; Shore, S. G. *Inorg. Chem.* **1989**, *28*, 3285.

Table IV. Selected Bond Distances and Angles for 4[a]

	(a) Bond Distances (Å)		
Au(1)-Au(2)	2.849 (1)	Au(1)-Ru(1)	2.728 (1)
Au(1)-P(1)	2.325 (3)	Au(1)-B	2.288 (15)
Au(2)-Ru(2)	2.730 (1)	Au(2)-P(2)	2.312 (3)
Au(2)-B	2.272 (13)	Ru(1)-Ru(3)	2.886 (1)
Ru(1)-Ru(4)	2.871 (1)	Ru(1)-B	2.130 (11)
Ru(1)-C(1)	1.929 (14)	Ru(1)-C(2)	1.876 (14)
Ru(1)-C(3)	1.923 (12)	Ru(2)-Ru(3)	2.913 (1)
Ru(2)-Ru(4)	2.864 (1)	Ru(2)-B	2.114 (13)
Ru(2)-C(4)	1.949 (14)	Ru(2)-C(5)	1.915 (13)
Ru(2)-C(6)	1.881 (12)	Ru(3)-Ru(4)	2.885 (1)
Ru(3)-B	2.259 (13)	Ru(3)-C(7)	1.933 (16)
Ru(3)-C(8)	1.920 (14)	Ru(3)-C(9)	1.903 (13)
Ru(4)-B	2.250 (14)	Ru(4)-C(10)	1.938 (16)
Ru(4)-C(11)	1.949 (13)	Ru(4)-C(12)	1.891 (13)
C(1)-O(1)	1.116 (17)	C(2)-O(2)	1.169 (17)
C(3)-O(3)	1.138 (15)	C(4)-O(4)	1.130 (19)
C(5)-O(5)	1.142 (16)	C(6)-O(6)	1.151 (16)
C(7)-O(7)	1.136 (20)	C(8)-O(8)	1.128 (17)
C(9)-O(9)	1.143 (17)	C(10)-O(10)	1.134 (21)
C(11)-O(11)	1.113 (17)	C(12)-O(12)	1.159 (17)
	(b) Bond Angles (deg)		
Au(2)-Au(1)-Ru-(1)	85.0 (1)	Au(2)-Au(1)-P(1)	118.6 (1)
Ru(1)-Au(1)-P-(1)	150.8 (1)	Au(2)-Au(1)-B	51.1 (3)
Ru(1)-Au(1)-B	49.3 (3)	P(1)-Au(1)-B	159.5 (3)
Au(1)-Au(2)-Ru(2)	87.4 (1)	Au(1)-Au(2)-P(2)	116.2 (1)
Ru(2)-Au(2)-P(2)	151.2 (1)	Au(1)-Au(2)-B	51.6 (4)
Ru(2)-Au(2)-B	49.0 (3)	P(2)-Au(2)-B	159.7 (3)
Au(1)-Ru(1)-Ru(3)	102.5 (1)	Au(1)-Ru(1)-Ru(4)	88.2 (1)
Au(2)-Ru(2)-Ru(4)	105.1 (1)	Ru(3)-Ru(2)-Ru(4)	59.9 (1)
Ru(1)-Ru(3)-Ru(2)	92.2 (1)	Ru(2)-Ru(3)-Ru(4)	59.2 (1)
Ru(1)-Ru(3)-Ru(4)	59.7 (1)	Ru(1)-Ru(4)-Ru(3)	60.2 (1)
Ru(1)-Ru(4)-Ru(2)	93.6 (1)	Ru(2)-Ru(4)-Ru(3)	60.9 (1)
Ru(3)-Ru(1)-Ru(4)	60.2 (1)	Ru(3)-Ru(2)-Ru(4)	59.9 (1)
Au(2)-Ru(2)-Ru(3)	71.7 (1)	Au(2)-Ru(2)-B	54.2 (4)
Ru(1)-Ru(4)-B	47.3 (3)	Au(1)-Ru(1)-B	54.5 (4)
Ru(3)-Ru(2)-B	50.4 (4)	Ru(4)-Ru(2)-B	51.1 (4)
Ru(3)-Ru(1)-B	50.9 (4)	Ru(4)-Ru(1)-B	50.9 (4)
Ru(2)-Ru(3)-B	46.1 (3)	Ru(1)-Ru(3)-B	47.0 (3)
Ru(4)-Ru(3)-B	50.1 (3)	Ru(2)-Ru(4)-B	47.0 (3)
Au(2)-B-Ru(4)	158.4 (7)	Ru(3)-Ru(4)-B	50.4 (3)
Au(1)-B-Au(2)	77.3 (5)	Au(1)-B-Ru(1)	76.2 (4)
Au(2)-B-Ru(1)	117.8 (6)	Au(1)-B-Ru(2)	122.2 (5)
Au(2)-B-Ru(2)	76.9 (4)	Ru(1)-B-Ru(2)	160.0 (8)
Au(1)-B-Ru(3)	148.9 (6)	Au(2)-B-Ru(3)	93.8 (5)
Ru(1)-B-Ru(3)	82.2 (4)	Ru(2)-B-Ru(3)	83.5 (5)
Au(1)-B-Ru(4)	118.4 (6)	Ru(1)-B-Ru(4)	81.9 (4)
Ru(2)-B-Ru(4)	82.0 (5)	Ru(3)-B-Ru(4)	79.6 (5)

[a] The labeling scheme is given in Figure 3.

Ru–H–B *endo*-hydrogen atoms is coupled to one ^{11}B nucleus. The $^{11}B\{^1H\}$ NMR spectrum becomes a triplet on coupling to protons (J_{BH} = 70 Hz) (part a vs part b of Figure 2), indicating that the two hydrogen atoms are attached to the boron atom. Both the ^1H and ^{11}B NMR chemical shifts for **1** compare favorably with those observed for **5** (Table I).

Compound **1** deprotonates readily via the loss of an Ru–H–B proton to give **2** (Chart I); the reaction proceeds in weakly basic media but most efficiently in the presence of sodium carbonate. From **1** to **2**, a downfield shift in the ^{11}B NMR spectrum (Table I) indicates an increase in the degree of direct Ru–B bonding, consistent with removal of a Ru–H–B rather than an Ru–H–Ru proton.[24,25] In support of this, the $^{11}B\{^1H\}$ NMR signal for **2** (Figure 2c) becomes a doublet (Figure 2d), with J_{BH} = 80 Hz. The difference in the ^{11}B shifts δ(anion) – δ(neutral), $\Delta\delta$, is strikingly similar for the tetraferraborane and the tetraruthenaborane (Table I); $\Delta\delta_{Fe}$ = 34 and $\Delta\delta_{Ru}$ = 32. Although the number of direct group 8 metal–boron interactions significantly alters the ^{11}B NMR chemical shift, the change from iron to ruthenium for a given pair of isostructural compounds does *not* greatly influence the position of the signal. We have observed a similar phenomenon when comparing ^{11}B NMR spectroscopic data for $Fe_3(CO)_9BH_5$ and $Ru_3(CO)_9BH_5$.[2]

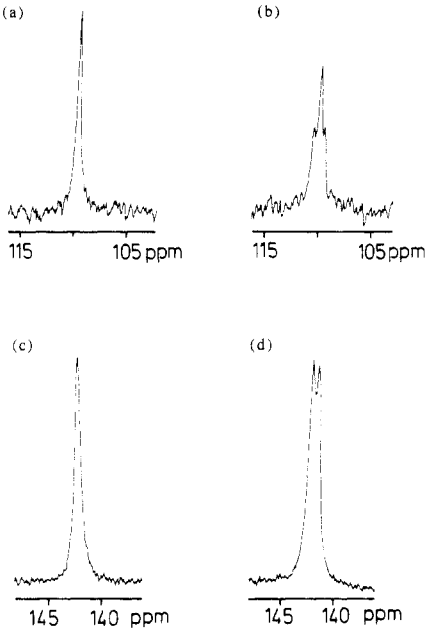

Figure 2. ^{11}B NMR spectra (128 MHz) of **1** and **2**: (a) $^{11}B\{^1H\}$ NMR spectrum of **1**; (b) proton-coupled ^{11}B NMR spectrum of **1**; (c) $^{11}B\{^1H\}$ NMR spectrum of **2**; (d) proton-coupled ^{11}B NMR spectrum of **2**.

The increase in metal–metal bond strengths on descending the iron triad is reflected in a increased energy barrier for the exchange of M–H–M and M–H–B *endo*-hydrogen atoms in the $[HM_4(CO)_{12}BH]^-$ anions on going from M = Fe to Ru. In the $[HFe_4(CO)_{12}BH]^-$ anion (**6**) a static structure is frozen out at temperatures ≤0 °C on the 300-MHz ^1H NMR time scale,[22] while for anion **2**, a static structure is observed at room temperature on the 250-MHz ^1H NMR time scale. A corresponding increase in the energy of activation for *endo*-hydrogen exchange is observed from $HFe_4(CO)_{12}CH$[26] to $HRu_4(CO)_{12}CH$;[4] these compounds are isoelectronic with **6** and **2**, respectively (see Chart II).

Clusters **1** and **2** are the final members of the series of iron and ruthenium butterfly clusters illustrated in Chart II. Each compound exhibits an M_4X (X = B, C) cluster core,[4,13,22,26-30] although only for compounds **5** and **14** have the structures been crystallographically confirmed.[13,24,28] In Chart II, the butterfly compounds are arranged in iso-

(24) Housecroft, C. E. *Polyhedron* **1987**, *6*, 1935.
(25) Fehlner, T. P.; Rath, N. P. *J. Am. Chem. Soc.* **1988**, *110*, 5345.
(26) Tachikawa, M.; Muetterties, E. L. *J. Am. Chem. Soc.* **1980**, *102*, 4541.
(27) Holt, E. M.; Whitmire, K. H.; Shriver, D. F. *J. Organomet. Chem.* **1981**, *213*, 125.
(28) Drezdon, M. A.; Whitmire, K. H.; Bhattacharyya, A. A.; Hsu, W.-L.; Nagel, C. C.; Shore, S. G.; Shriver, D. F. *J. Am. Chem. Soc.* **1982**, *104*, 5630.
(29) Drezdon, M. A.; Shriver, D. F. *J. Mol. Catal.* **1983**, *21*, 81.
(30) Beno, M. A.; Williams, J. M.; Tachikawa, M.; Muetterties, E. L. *J. Am. Chem. Soc.* **1981**, *103*, 1485.

Chart II

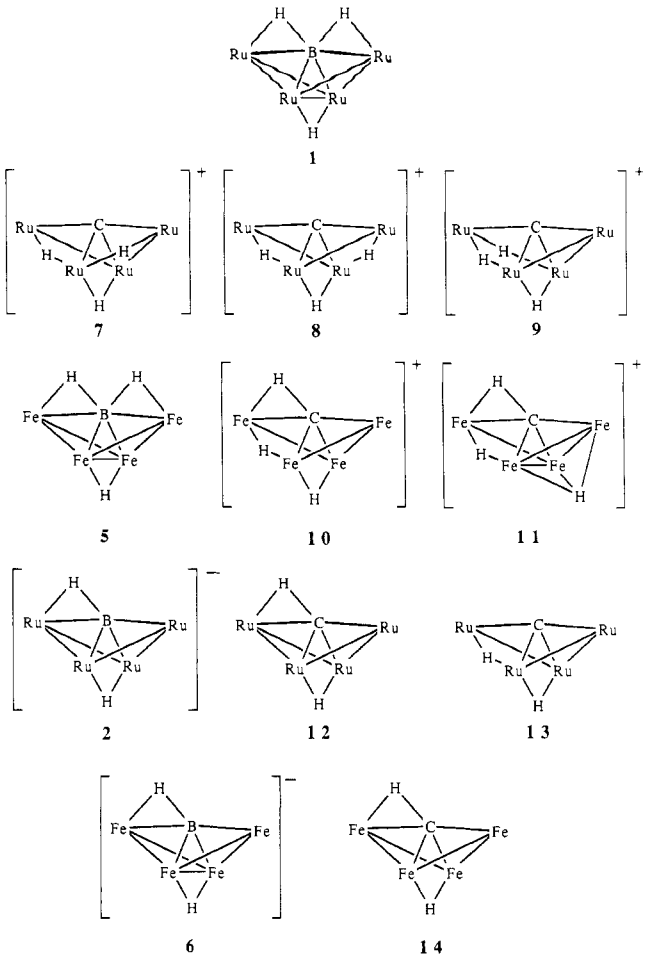

electronic pairs; isoelectronic with **1** is the $[H_3Ru_4(CO)_{12}C]^+$ cation, for which two isomers exist, and three possible structures, **7–9**, have been proposed.[4] Irrespective of the precise locations of the *endo*-hydrogen atoms in the cation, the general observation is that, from $HRu_4(CO)_{12}BH_2$ to $[H_3Ru_4(CO)_{12}C]^+$, Ru–H–Ru interactions become more favorable than Ru–H–X (X = B, C) bridges. As the cluster becomes more positively charged, the ruthenium valence shell (particularly 4d) orbitals will contract, allowing them to overlap more effectively with the hydrogen 1s AO's. The same preference, although less pronounced, is observed if we compare **2** with $H_2Ru_4(CO)_{12}C$; anion **2** possesses one Ru–H–B and one Ru–H–Ru interaction, while in $H_2Ru_4(CO)_{12}C$, ~85% exists as an isomer, **13**, with two Ru–H–Ru interactions and a second isomer, **12**, is isostructural with **2**.[4] Comparing each ruthenium compound with its respective iron analogue (viz. **2** with **6**, and **12** and **13** with **14**), we see that while the metallaborane clusters retain their preference for M–H–B over M–H–M interactions, the ruthenium carbon-containing clusters show a greater tendency to form Ru–H–Ru bridges than do the iron clusters to form Fe–H–Fe interactions. These trends may be rationalized in terms of the relative M–H–M and M–H–X (M = Fe, Ru; X = B, C) bond strengths and in terms of arguments put forward by Fehlner et al.[31] Efficient overlap of an *endo*-hydrogen atom with a cluster edge or face is only achieved when there is a region of electron density lying *outside* the cluster. Thus from B to C, as valence shell AO's contract, the *endo*-hydrogen atoms migrate toward the metal framework rather than be associated with the main-group atom.

(31) Lynam, M. M.; Chipman, D. M.; Barreto, R. D.; Fehlner, T. P. *Organometallics* **1987**, *6*, 2405.

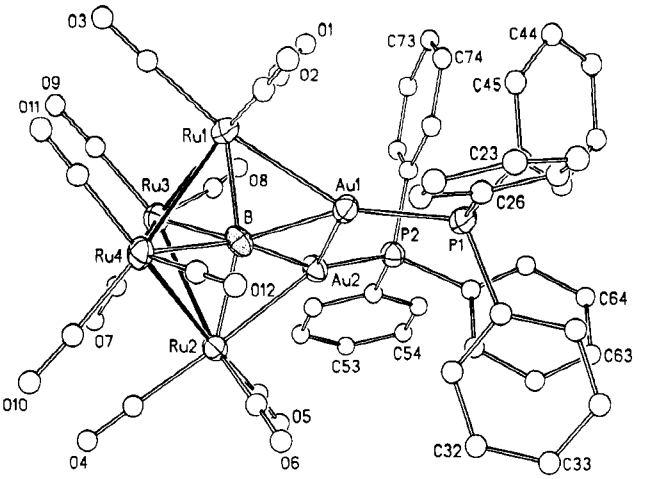

Figure 3. Molecular structure and numbering scheme for **4**. Hydrogen atoms are not shown.

Reactions of 2 with Ph_3PAuCl. The anion **2** reacts with 1 equiv of Ph_3PAuCl to form the gold(I) phosphine derivative **3**, which has been spectroscopically characterized. The retention of a tetraruthenium butterfly framework is supported by a crystal structure of the digold derivative **4** (see below) and from our previous observations that, in the reaction of $[HFe_4(CO)_{12}BH]^-$ with gold(I) phosphines, the metal butterfly cluster core is resistant to structural change.[15] The ^{11}B NMR spectrum of **3** is close to that observed for anion **2**, implying that the environment around the boron atom is little changed in going from **2** to **3**. As expected,[15,32,33] the formation of an Au–B bond has an insignificant effect upon the ^{11}B NMR chemical shift. In the ^1H NMR spectrum, resonances attributable to Ru–H–B and Ru–H–Ru interactions are observed. Hence, a structure for **3** is proposed in which a $AuPPh_3$ fragment bridges an Ru_{wing}–B edge (Chart I).

The reaction of anion **2** with ≥2 equiv of Ph_3PAuCl leads to the formation of the digold derivative **4**. Spectroscopic characterization of this cluster implies that the boron atom has become encapsulated within the metal cage; a downfield singlet (δ +170) is observed in the ^{11}B NMR spectrum, and a single high-field resonance in the ^1H NMR spectrum at δ −20.66 indicates the presence of an Ru–H–Ru bridge. These expectations are confirmed by a crystallographic study of **4**.

Molecular Structure of 4. The molecular structure of **4** is illustrated in Figure 3, and bond distances and angles are listed in Table IV. The cluster possesses a tetraruthenium butterfly framework with an internal dihedral angle of 117.4 (1)°. The boron atom is in a μ_4-bonding mode with respect to the tetraruthenium butterfly and is at an elevation of 0.37 (1) Å above the Ru(1)---Ru(2) vector, (i.e. above a line drawn between the wingtip atoms of the butterfly). In comparing the structural parameters of the Ru_4B core in **4** with those of the Fe_4B core in similar compounds,[14,15,34] we note that the internal dihedral angle of the butterfly opens slightly (113.5 ± 0.5° for Fe_4B to 117.4° in **4**), to accommodate the boron atom within the M_4 framework as the transition-metal radius increases from Fe to Ru; the boron atom does not rise significantly out of the butterfly (0.34 ± 0.03° for Fe_4B to 0.37° in **4**). Each

(32) Harpp, K. S.; Housecroft, C. E. *J. Organomet. Chem.* **1988**, *340*, 389.

(33) Housecroft, C. E.; Rheingold, A. L. *J. Am. Chem. Soc.* **1986**, *108*, 6420.

(34) Housecroft, C. E.; Rheingold, A. L.; Shongwe, M. S. *Organometallics* **1988**, *7*, 1885.

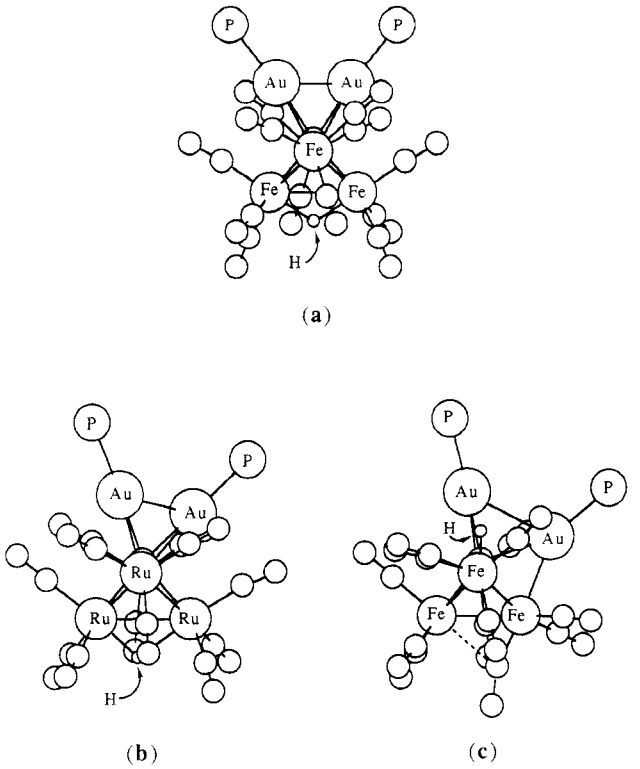

Figure 4. Structures of (a) $HFe_4(CO)_{12}Au_2(PEt_3)_2B$, (b) $HRu_4(CO)_{12}Au_2(PPh_3)_2B$, and (c) $Fe_4(CO)_{12}Au_2(PPh_3)_2BH$, each viewed along the M_{wing}–M_{wing} vector (M = Fe, Ru). The H position has, in each case, not been directly located.

$AuPPh_3$ fragment bridges one Ru_{wing}–B edge, and the Au–B distances of 2.288 (15) and 2.272 (13) Å are similar to corresponding bond lengths observed in related aura-ferraborane clusters.[14,15,33-36] The boron atom is therefore within bonding distance of all six metal atoms, and this observation is consistent with the observed downfield ^{11}B NMR chemical shift; i.e., the boron atom experiences a boridic rather than a borane environment. The hexametal atom core is nonoctahedral, with the two gold atoms skewed across the open face of the Ru_4B butterfly core (Figure 3). A similar geometry has been observed in $HFe_4(CO)_{12}Au_2(PEt_3)_2B$,[15,34] although, in **4**, the planes containing the Au(1)–Au(2) and Ru(3)–Ru(4) vectors are not parallel as is evident from Figure 4b; ∠Ru(3)BAu(2) = 93.8 (5)° and ∠Ru(4)BAu(1) = 118.4 (6)°. The significance of the tilting of the $\{(PPh_3)_2Au_2\}$ unit with respect to the $\{HRu_4(CO)_{12}B\}$ core is discussed below.

The carbonyl ligands in **4** are all terminally attached. If we ignore the Ru–B interactions, each wingtip Ru atom is in an approximately octahedral environment. The metal hydride was not located directly, but the orientations of the carbonyl ligands on the hinge Ru atoms (Figure 3) indicate the presence of an Ru(3)–H–Ru(4) bridging hydrogen atom, consistent with the observation of a metal hydride ^1H NMR spectral resonance (δ −20.66).

Cluster **4** is isoelectronic[37] with the tetraruthenium butterfly cluster $Ru_4(CO)_{12}Au_2(PMe_2Ph)_2C$,[38] but it is significant that the clusters are not isostructural. In the carbido cluster, both in the solid state and in solution, one $AuPMe_2Ph$ moiety bridges the Ru_{hinge}–Ru_{hinge} bond while the second interacts with *both* Ru_{wing} atoms and with the carbido atom to form a symmetrical bridge. The change from C to BH as one goes from $Ru_4(CO)_{12}Au_2(PMe_2Ph)_2C$ to compound **4** clearly introduces the question of placement of three instead of two electrophiles on the surface of the Ru_4X cluster core. We have previously suggested that a charge effect may be responsible for driving the gold(I) phosphines to seek preferential interaction with M–B rather than M–M edges.[14] This effect will be more pronounced in a metallaborido than in a metallacarbido cluster, as the effective nuclear charge increases in going from B to C, contracting the valence shell orbitals on the main-group atom. Perhaps significantly, the same structural trends are emerging with the aura butterfly clusters as with the hydrido butterfly species illustrated in Chart II. Besides the observation of a greater preference for X–Au(PR_3)–Ru over Ru–Au(PR_3)–Ru interactions from X = C to B, a change from Fe to Ru in $M_4(CO)_{12}Au_2(PR_3)_2C$ appears to favor M–Au(PR_3)–M over C–Au(PR_3)–M interactions.[38,39] A note of caution should, however, be added since, for the metallacarbides, we are comparing systems with different phosphine substituents (see below).

Comparison of 4 with $HFe_4(CO)_{12}Au_2(PR_3)_2B$. Recently, we presented a detailed study of the structural isomerism exhibited by compounds of type $HFe_4(CO)_{12}Au_2(PR_3)_2B$ (R = alkyl, aryl).[15,34] With the constraint of a structurally invariant (proven by crystallographic characterization)[14,15,34] Fe_4 butterfly framework, the locations of the two gold(I) phosphine fragments vary depending upon the steric requirements of the phosphine substituents. The characterization of the tetraruthenium cluster **4** adds another dimension to our steric arguments; corresponding views of the structures of $HFe_4(CO)_{12}Au_2(PEt_3)_2B$, cluster **4**, and $Fe_4(CO)_{12}Au_2(PPh_3)_2BH$ are shown in Figure 4. The unusual geometry of the Fe_4Au_2B core in $Fe_4(CO)_{12}Au_2(PPh_3)_2BH$ (Figure 4c) compared to the more symmetrical core structure in $HFe_4(CO)_{12}Au_2(PEt_3)_2B$ (Figure 4a) has been attributed to the greater cone angle of $AuPPh_3$ vs that of $AuPEt_3$.[15] As one goes from $Fe_4(CO)_{12}Au_2(PPh_3)_2BH$ to its ruthenium analogue **4**, the metal butterfly opens up sufficiently to overcome the steric crowding experienced by the two $AuPPh_3$ fragments in the tetrairon cluster. Hence, the structure of **4** is more closely related to that of $HFe_4(CO)_{12}Au_2(PEt_3)_2B$ than to $Fe_4(CO)_{12}Au_2(PPh_3)_2BH$. However, careful inspection of parts a and b of Figure 4 illustrates that the relief of steric strain is not sufficient to allow cluster **4** to attain C_2 symmetry. In fact, the structure of **4** appears to lie partway along a path, previously postulated,[15] that converts the M_4Au_2B core in $HFe_4(CO)_{12}Au_2(PEt_3)_2B$ to that in $Fe_4(CO)_{12}Au_2(PPh_3)_2BH$. Changes in the hinge atom carbonyl ligand orientations further support this suggestion. From Figure 4a through to Figure 4c, one $AuPR_3$ moiety migrates from a B–Au(PR_3)–M_{wing} to a B–Au(PR_3)–M_{hinge} bridging site; coupled with this change is a rotation of the associated hinge $M(CO)_3$ unit. The greater the degree of tilting of the $\{(PR_3)_2Au_2\}$ unit with respect to the $\{HM_4(CO)_{12}B\}$ core, the further the hinge carbonyl ligands rotate, until, eventually, as the B–Au(PR_3)–M_{hinge} interaction forms at the expense of the B–Au(PR_3)–M_{wing} bridge, one CO ligand forces the M–H–M hydride out of its bridging site (Figure 4c).

(35) Harpp, K. S.; Housecroft, C. E.; Rheingold, A. L.; Shongwe, M. S. *J. Chem. Soc., Chem. Commun.* **1988**, 965.
(36) Housecroft, C. E.; Rheingold, A. L.; Shongwe, M. S. *J. Chem. Soc., Chem. Commun.* **1988**, 1630.
(37) The term *isoelectronic* is used here to relate the clusters $Ru_4(CO)_{12}Au_2L_2C$ and $HRu_4(CO)_{12}Au_2L_2B$; the phosphine substituents in the two compounds are not identical, but this does not affect the number of *cluster* bonding electrons.
(38) Cowie, A. G.; Johnson, B. F. G.; Lewis, J.; Raithby, P. R. *J. Chem. Soc., Chem. Commun.* **1984**, 1710.
(39) Johnson, B. F. G.; Kaner, D. A.; Lewis, J.; Raithby, P. R.; Rosales, M. J. *J. Organomet. Chem.* **1982**, *231*, C59.
(40) Sheldrick, G. *SHELXTL (5.1)*; Nicolet XRD Corp.: Madison, WI.

Acknowledgment is made to the donors of the Petroleum Research Fund, administered by the American Chemical Society, for support of this research, to the Royal Society for a 1983 University Research Fellowship (to C.E.H.), and to the NSF for a grant toward the purchase of a diffractometer at the University of Delaware. Johnson-Matthey is thanked for generous loans of $RuCl_3$.

Supplementary Material Available: Tables of atomic coordinates, bond distances, bond angles, thermal parameters, and H atom coordinates (9 pages); a listing of structure factors (41 pages). Ordering information is given on any current masthead page.

Use of Palladium-Catalyzed Coupling Reactions in the Synthesis of Heterobimetallic Complexes. Preparation of Bis(cyclopentadienyl)acetylene Heterodinuclear Complexes

Claudio Lo Sterzo† and J. K. Stille*

Department of Chemistry, Colorado State University, Fort Collins, Colorado 80523

Received July 28, 1989

The palladium-catalyzed coupling reactions of η^5-iodocyclopentadienyl complexes of Fe, W, Mn, and Re with $Bu_3SnC{\equiv}CH$ yield the corresponding η^5-ethynylcyclopentadienyl derivatives $(\eta^5\text{-}HC{\equiv}CC_5H_4)ML_n$ (M = Fe, W, Mn, Re). Upon reaction with Et_2NSnR_3 (R = Me, Bu), the acetylenic proton is replaced with a trialkyltin group, forming the η^5-[(trialkylstannyl)ethynyl]cyclopentadienyl derivatives $(\eta^5\text{-}R_3SnC{\equiv}CC_5H_4)ML_n$. A second palladium-catalyzed coupling reaction between these trialkyltin derivatives and (η^5-iodocyclopentadienyl)metal complexes affords the heterobimetallic complexes $L_nM(\eta^5\text{-}C_5H_4)C{\equiv}C(\eta^5\text{-}C_5H_4)M'L_m$ (M and M′ = Fe, W, Mo, Mn, Re). The crystal structure of $Ph_3P(CO)_2Mn(\eta^5\text{-}C_5H_4)C{\equiv}C(\eta^5\text{-}C_5H_4)W(CO)_3CH_3$ confirmed the general structure of these heterobimetallic complexes and showed that the two metals attached to the cyclopentadienyl rings were pointed in opposite directions.

Introduction

One goal of research directed toward the efficient reduction of carbon monoxide by homogeneous catalysis has been the preparation of mixed-metal complexes containing both "early" and "late" transition metals.[1] Much of the interest in this chemistry is due to the expectation that the two metal centers will interact cooperatively in a catalytic process to affect novel reactions and increase the overall reaction rates under mild reaction conditions.[2] One approach to this goal has been to design an appropriate bridging ligand that holds the two metal centers in close proximity, thus allowing effective interaction (i.e., exchange of ligands) during the catalytic cycle. In such a dinuclear complex, either of the two metals may separately catalyze two consecutive reactions, or both metals may simultaneously perform some transformation through interaction with the substrate.

Most of the bidentate ligands used to bring two metal centers together are bridging ligands bearing two coordinating centers, P, As, N, S, or O, linked in the same molecule in various ways.[3] The limitation in the use of such ligands resides in the limited thermal stability of their metal complexes due to the relatively weak metal–ligand bond. By contrast, cyclopentadienyl ligands have much stronger ligand–metal bonds (60–70 kcal mol^{-1} for typical η^5-cyclopentadienyl–metal bonds versus 30–40 kcal mol^{-1} for a trialkylphosphine–metal bond).[4] However, general synthetic routes for the synthesis of heterobimetallic complexes held together by two covalently linked cyclopentadienide rings are difficult. While a number of homobimetallic structures in which two identical metal centers are complexed by the cyclopentadienyl rings of dicyclopentadienylmethane,[5] dicyclopentadienyldimethylsilane,[6] dicyclopentadienylacetylene,[7,8] and fulval-

* Deceased. Address all correspondence to Dr. Louis S. Hegedus at Colorado State University.

† Present address: Centro C.N.R. di Studio sui Meccanismi di Reazione, Dipartimento di Chimica, Univ. "La Sapienza", P. le A. Moro, 2 00185 Roma, Italy.

(1) (a) Bruce, M. I. *J. Organomet. Chem.* **1983**, *242*, 147. (b) Roberts, D. A.; Geoffroy, G. L. In *Comprehensive Organometallic Chemistry*; Wilkinson, G., Stone, F. G. A., Abel, E. W., Eds.; Pergamon Press: Oxford, 1982; Vol. 6, p 763. (c) Gladfelter, W. L.; Geoffroy, G. L. *Adv. Organomt. Chem.* **1980**, *18*, 207.

(2) (a) Muetterties, E. L.; Krause, M. J. *Angew. Chem., Int. Ed. Engl.* **1983**, *22*, 135. (b) Muetterties, E. L.; Rhodin, T. N.; Band, E.; Brucker, C. F.; Pretzer, W. R. *Chem. Rev.* **1979**, *79*, 91. (c) Band, E.; Muetterties, E. L. *Chem. Rev.* **1978**, *78*, 639. (d) Muetterties, E. L. *Science* **1977**, *196*, 839. (e) Muetterties, E. L. *Bull. Soc. Chim. Belg.* **1975**, *84*, 959.

(3) (a) Maitlis, P. M.; Espinet, P.; Russell, M. J. H. In *Comprehensive Organometallic Chemistry*; Wilkinson, G., Stone, F. G. A., Abel, E. W., Eds.; Pergamon Press: New York, 1982; Vol. 6, p 265. (b) Arnold, D. P.; Bennett, M. A.; McLaughlin, G. M.; Robertson, G. B.; Whittaker, M. J. *J. Chem. Soc., Chem. Commun.* **1983**, 32. (c) Puddephatt, R. J.; Thompson, P. J. *J. Organomet. Chem.* **1976**, *117*, 395. (d) Ebsworth, E. A. V.; Ferrier, H. M.; Henner, B. J. L.; Rankin, D. W. H.; Reed, F. J. S.; Robertson, H. E.; Whitelock, J. D. *Angew. Chem., Int. Ed. Engl.* **1977**, *16*, 482. (e) Richter, U.; Vahrenkamp, H. *J. Chem. Res., Synop.* **1977**, 156. (f) Köpf, H.; Räthlein, K. H. *Angew. Chem., Int. Ed. Engl.* **1969**, *8*, 980. (g) Braterman, P. S.; Wilson, V. A.; Joshi, K. K. *J. Chem. Soc. A* **1971**, 191. (h) Hughes, R. P. In *Comprehensive Organometallic Chemistry*; Wilkinson, G., Stone, F. G. A., Abel, E. W., Eds.; Pergamon Press: New York, 1982; Vol. 5, p 277.

(4) Connor, J. A. *Top. Curr. Chem.* **1976**, *71*, 71.

(5) (a) Bryndza, H. E.; Berman, R. G. *J. Am. Chem. Soc.* **1979**, *101*, 4766. (b) Mueller-Westerhoff, U. T.; Nazzal, A.; Tanner, M. *J. Organomet. Chem.* **1982**, *236*, C41. (c) Scholz, H. J.; Werner, H. *J. Organomet. Chem.* **1986**, *303*, C8.

(6) (a) Day, V. W.; Thompson, M. R.; Nelson, G. O.; Wright, M. E. *Organometallics* **1983**, *2*, 494. (b) Nelson, G. O.; Wright, M. E. *Ibid.* **1982**, *1*, 565. (c) Nelson, G. O.; Wright, M. E. *J. Organomet. Chem.* **1982**, *239*, 353. (d) Wegner, P. A.; Uski, V. A.; Kiester, R. P.; Dabestani, S.; Day, V. W. *J. Am. Chem. Soc.* **1977**, *99*, 4846. (e) Weaver, J.; Woodward, P. *J. Chem. Soc., Dalton Trans.* **1973**, 1439. (f) Wright, M. E.; Mezza, T. M.; Nelson, G. O.; Armstrong, N. R.; Day, V. W.; Thompson, M. R. *Organometallics* **1983**, *2*, 1711.

(7) Bunel, E. E.; Valle, L.; Jones, N. L.; Carroll, P. J.; Gonzalez, M.; Munoz, N.; Manriquez, J. M. *Organometallics* **1988**, *7*, 789.

0276-7333/90/2309-0687$02.50/0